

Superlight small pairs in face-centered-cubic extended Hubbard models

Ganiyu D. Adebanjo,¹ P.E. Kornilovitch,² and J.P. Hague¹

¹*School of Physical Sciences, The Open University, Walton Hall, Milton Keynes, MK7 6AA, UK*

²*Department of Physics, Oregon State University, Corvallis, OR, 97331, USA*

(Dated: July 22, 2022)

We exactly solve a two-particle *UV* model to explore the behavior of pairs in a face-centered cubic (FCC) lattice within an extended Hubbard model. The conditions for pair formation, pair mass, pair size, and the Bose-Einstein condensation (BEC) temperature are examined. Our results show that strongly bound, superlight and small pairs can be generated in the FCC lattice, which are much lighter than pairs in other 3D lattices. We estimate that such pairs can Bose condense at high temperatures even if the lattice constant is large. Therefore, in the search for materials with high superconducting transition temperatures, three-dimensional materials with an underlying FCC structure should be investigated due to the possibility of superlight small pairs.

I. INTRODUCTION

There are a number of low-dimensional systems within which superlight pair states can be realised, for example the staggered ladder [1], triangular lattice [2, 3] and quasi-two-dimensional hexagonal lattice [4]. Superlight pairs consist of two fermions bound onto neighbouring sites by a combination of strong intersite attraction and strong onsite repulsion. Such pairs can be light and small if it is possible to move to neighboring lattice sites via a single hop without breaking the pairing [1], so that the pair motion is a first order effect. In many materials there is a strong onsite Coulomb repulsion, so intersite pairs are formed via any intersite or long-range attraction, which could originate either from phonons or other more exotic mechanisms. Localized light states are of interest because of their potential to form Bose-Einstein condensates (BEC) at high temperatures.

Extended Hubbard models [5, 6] contain the essential interactions to realize superlight states. The Hamiltonian of an extended Hubbard model is defined as:

$$H = \sum_{\langle \mathbf{n}, \mathbf{a} \rangle \sigma} t_{\mathbf{a}} c_{\mathbf{n}+\mathbf{a}, \sigma}^\dagger c_{\mathbf{n}\sigma} + U \sum_{\mathbf{n}} \hat{\rho}_{\mathbf{n}\uparrow} \hat{\rho}_{\mathbf{n}\downarrow} + \sum_{\langle \mathbf{n}, \mathbf{a} \rangle} V \hat{\rho}_{\mathbf{n}+\mathbf{a}} \hat{\rho}_{\mathbf{n}} \quad (1)$$

where $c_{\mathbf{n}\sigma}^\dagger$ ($c_{\mathbf{n}\sigma}$) creates (annihilates) an electron of spin σ at site \mathbf{n} , $\hat{\rho}_{\mathbf{n}} = \hat{\rho}_{\mathbf{n}\uparrow} + \hat{\rho}_{\mathbf{n}\downarrow}$, where $\hat{\rho}_{\mathbf{n}\sigma}$ is the number operator for electrons on site \mathbf{n} with spin σ , \mathbf{a} is the intersite lattice vector, $t_{\mathbf{a}}$ is the intersite hopping, U is the onsite interaction and V is the intersite interaction. Both U and V may be attractive or repulsive, although in most materials repulsive U is more likely due to the difficulties of overcoming the Hubbard U with attractive interactions, such as those due to electron-phonon interactions. In the low-density limit the model is also known as the *UV* model. Properties of local pairs, which can be used to estimate the Bose-Einstein condensation temperature, have been studied in simple systems using the *UV* model [4, 7–10]. If U is highly repulsive and V is attractive, then exceptionally mobile pairs (superlight states) can be realized on suitable lattices.

In the context of superlight small pairs, the face-centered cubic (FCC) lattice can be viewed as the 3D

analogue of the 2D triangular lattice, in that electrons paired between near-neighbor sites can move with a single hop. This remarkable feature should result in a low effective pair mass which could in turn yield a higher transition temperature relative to other systems that lack it. This implies that electron pairing in the FCC lattice is a candidate for obtaining superlight states. To our knowledge, superlight pairs have not yet been examined in FCC systems. The complexity of the FCC lattice structure and increased number of nearest-neighbor sites complicate the calculation and we aim to fill this gap. An illustration of the superlight pair movement in an FCC lattice is shown in Fig. 1. As long as the intersite attraction is maintained, and there is sufficient Hubbard U to suppress on-site pairing, the pair can move easily through the lattice.

In spite of their ubiquity in condensed matter systems, FCC lattices are often overlooked within the correlated electrons community owing to their relative complexity compared to other lattices. Materials of interest with FCC lattices include the A_3C_{60} compounds: a family of molecular compounds with high transition temperature [11] (where A is an alkali metal e.g. K, Rb, Cs) which are predominantly FCC structured [12]. In addition to electron-phonon interactions [11] found in these alkali-doped compounds, strong correlation [13] is also prevalent. The presence of long-range phonon mediated interactions (e.g. the intermolecular modes [12, 14]) may lead to suitable conditions for extended Hubbard physics and superlight pairs, and even if they do not have a role in those compounds, might be relevant to other FCC materials.

This work aims to provide an exact solution of the two-electron problem in an FCC lattice. We calculate the critical potentials U_c (V_c) to bind particles into pairs, the system's total energy, the pair's size and mass, and BEC transition temperatures of pairs in the low-density (dilute) limit. The paper is organized as follows: We describe the model Hamiltonian and methodology used to solve the *UV* model in the dilute limit (Sec. II). In Sec. III, the properties of the formed pairs are reported. We conclude this work with a discussion in Sec. IV.

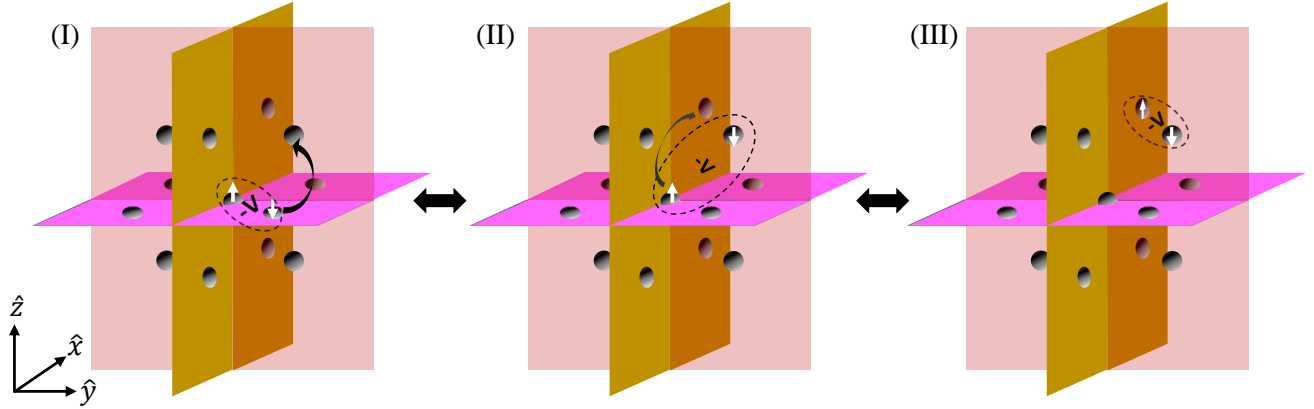


FIG. 1: [Color online] Schematic demonstrating the first-order hopping of superlight small pairs on the FCC lattice. The white vertical arrow represents an electron with its spin, each small gray circle is a lattice site (only the 13 sites of interest are shown), the dashed oval represents a bound state through an attractive V , the curved arrow represents electron hopping, and the two-way arrow implies that the configurations are degenerate. The key feature here is that the pair is itinerant as long as the intersite interaction is sufficiently attractive, and there is sufficient Hubbard U to stop on-site pairs from forming. Unlike in other cubic lattices where first-order superlight states are only attainable via an attractive U , superlight state in the FCC lattice corresponds to a more physical case where the local Coulomb repulsion is large.

II. METHODOLOGY

We find exact solution to a single-orbital system of two spin 1/2 fermions where the orbital energy is taken to be zero. The two-body problem relevant to the Hamiltonian in Eqn. (1) must satisfy the equation below:

$$\begin{aligned} & \sum_{\mathbf{a}} t_{\mathbf{a}} [\Psi(\mathbf{n}_1 + \mathbf{a}, \mathbf{n}_2) \\ & + \Psi(\mathbf{n}_1, \mathbf{n}_2 + \mathbf{a})] + \sum_{\mathbf{a}} \hat{V}_{\mathbf{a}} \delta_{\mathbf{n}_1 - \mathbf{n}_2, \mathbf{a}} \Psi(\mathbf{n}_1, \mathbf{n}_2) \\ & = E \Psi(\mathbf{n}_1, \mathbf{n}_2) \end{aligned} \quad (2)$$

Here E is the total energy of the system and $\Psi(\mathbf{n}_1, \mathbf{n}_2)$ is the real-space wave function of the fermions. $\hat{V}_{\mathbf{a}}$ combines the interaction terms into a single function with $\hat{V}_{r=0} = U$ and $\hat{V}_{r=\mathbf{a}} = V$. The wave function in Fourier space is

$$\psi_{\mathbf{k}_1 \mathbf{k}_2} = \frac{1}{N} \sum_{\mathbf{n}_1 \mathbf{n}_2} \Psi(\mathbf{n}_1, \mathbf{n}_2) e^{-i\mathbf{k}_1 \mathbf{n}_1 - i\mathbf{k}_2 \mathbf{n}_2} \quad (3)$$

where N is the total number of lattice points. Substituting the inverse of Eqn. (3) into Eqn. (2) gives:

$$(E - \varepsilon_{\mathbf{k}_1} - \varepsilon_{\mathbf{k}_2}) \psi_{\mathbf{k}_1 \mathbf{k}_2} = \frac{1}{N} \sum_{\mathbf{a} \mathbf{q}} \hat{V}_{\mathbf{a}} e^{i(\mathbf{q} - \mathbf{k}_1) \mathbf{a}} \psi_{\mathbf{q}, \mathbf{k}_1 + \mathbf{k}_2 - \mathbf{q}}. \quad (4)$$

where \mathbf{k} is the particle's momentum vector. The dispersion relation in the FCC lattice is given as

$$\begin{aligned} \varepsilon_{\mathbf{k}} = -4t \left[\cos \frac{k_x b}{2} \cdot \cos \frac{k_y b}{2} + \cos \frac{k_y b}{2} \cdot \cos \frac{k_z b}{2} \right. \\ \left. + \cos \frac{k_x b}{2} \cdot \cos \frac{k_z b}{2} \right] \end{aligned} \quad (5)$$

where b is the lattice constant.

The solution to the problem involves 13 self-consistent algebraic equations. We apply (anti-)symmetrization to separate the symmetric (singlet) states from the anti-symmetric (triplet) states. Following Ref. 10, the (anti-)symmetrized wave function is expressed as

$$\begin{aligned} & (E - \varepsilon_{\mathbf{k}_1} - \varepsilon_{\mathbf{k}_2}) \phi_{\mathbf{k}_1 \mathbf{k}_2}^{\pm} \\ & = \frac{1}{N} \sum'_{\mathbf{q} \mathbf{a}} \hat{V}_{\mathbf{a}} \left\{ e^{i(\mathbf{q} - \mathbf{k}_1) \mathbf{a}} \pm e^{i(\mathbf{q} - \mathbf{k}_2) \mathbf{a}} \right\} \phi_{\mathbf{q}, \mathbf{k}_1 + \mathbf{k}_2 - \mathbf{q}}^{\pm} \end{aligned} \quad (6)$$

where

$$\phi_{\mathbf{k}_1 \mathbf{k}_2}^{\pm} = \psi_{\mathbf{k}_1 \mathbf{k}_2} \pm \psi_{\mathbf{k}_2 \mathbf{k}_1}, \quad (7)$$

and $+$ and $-$ refer to the singlet and the triplet wave functions, respectively. The summation over the lattice vector, \mathbf{a} , in Eqn. (6) is split into two sets: $\{\mathbf{a}_+\}$ for singlets, and $\{\mathbf{a}_-\}$ for triplets. We define them as

$$\{\mathbf{a}_+\} = \left\{ (0, 0, 0), \left(\frac{b}{2}, \frac{b}{2}, 0\right), \left(0, \frac{b}{2}, \frac{b}{2}\right), \left(\frac{b}{2}, 0, \frac{b}{2}\right), \right. \\ \left. \left(\frac{b}{2}, -\frac{b}{2}, 0\right), \left(0, \frac{b}{2}, -\frac{b}{2}\right), \left(-\frac{b}{2}, 0, \frac{b}{2}\right) \right\} \quad (8)$$

$$\{\mathbf{a}_-\} = \left\{ \left(\frac{b}{2}, \frac{b}{2}, 0\right), \left(0, \frac{b}{2}, \frac{b}{2}\right), \left(\frac{b}{2}, 0, \frac{b}{2}\right), \left(\frac{b}{2}, -\frac{b}{2}, 0\right), \right. \\ \left. \left(0, \frac{b}{2}, -\frac{b}{2}\right), \left(-\frac{b}{2}, 0, \frac{b}{2}\right) \right\} \quad (9)$$

$$\left(0, \frac{b}{2}, -\frac{b}{2}\right), \left(-\frac{b}{2}, 0, \frac{b}{2}\right) \quad (10)$$

where, again, b is the lattice constant. The primed summation in Eqn. (6) means that a factor of 1/2 should be included for the case $\mathbf{a}_+ = 0$. If we define a function

$$\Phi_{\mathbf{a}_{\pm}}^{\pm}(\mathbf{k}_1 + \mathbf{k}_2) = \Phi_{\mathbf{a}_{\pm}}^{\pm}(\mathbf{P}) \equiv \frac{1}{N} \sum_{\mathbf{q}} e^{i\mathbf{q}\mathbf{a}_{\pm}} \phi_{\mathbf{q}, \mathbf{P} - \mathbf{q}}^{\pm} \quad (11)$$

where $\mathbf{P} = \mathbf{k}_1 + \mathbf{k}_2$ is the total momentum of the particle pair, then, $\phi_{\mathbf{k}_1 \mathbf{k}_2}^\pm$ in Eqn. (6) can be expressed in terms of $\Phi_{\mathbf{a}_\pm}^\pm$. Replacing $\phi_{\mathbf{q}, \mathbf{P} - \mathbf{q}}^\pm$ in Eqn. (11) leads to the self-consistent equations

$$\Phi_{\mathbf{a}_\pm}^\pm(\mathbf{P}) = - \sum_{\mathbf{a}'_\pm} \hat{V}_{\mathbf{a}_\pm} L_{\mathbf{a}_\pm \mathbf{a}'_\pm}^\pm(E, \mathbf{P}) \Phi_{\mathbf{a}'_\pm}^\pm(\mathbf{P}) \quad (12)$$

where

$$L_{\mathbf{a}_\pm \mathbf{a}'_\pm}^\pm(E, \mathbf{P}) = \frac{1}{N} \sum_{\mathbf{q}} \frac{e^{i\mathbf{q}(\mathbf{a}_\pm - \mathbf{a}'_\pm)} \pm e^{i[\mathbf{q}\mathbf{a}_\pm - (\mathbf{P} - \mathbf{q})\mathbf{a}'_\pm]}}{-E + \varepsilon_{\mathbf{q}} + \varepsilon_{\mathbf{P} - \mathbf{q}}} \quad (13)$$

is the Green's function of the lattice. The full dispersion matrices for the singlets and triplets can be found in Appendix A and all calculations are at zero temperature.

III. RESULTS

A. Total Energy

The ground state energy can be used to identify whether two particles are bound or not. At zero momentum and zero temperature, the threshold energy of two unbound particles is $E^{\text{Th}} = -2W$, where $W = 12t$ is the half-bandwidth. The total energy in Fig. 2 shows all the different pair symmetries found in the FCC lattice. The particles are unbound when there is a plateau at $-2W$ and the energy drops below this threshold value when the particles bind.

A critical attraction must be reached before the formation of any bound state. At very large attractions U and V , the s -states have very similar values (insets of Fig. 2a and 2b). In Fig. 2b, the s -states are formed at relatively weak intersite attractions V compared to other states. Additionally, for very strong attractive V , the energies of all the pair symmetries are separated by an energy of order t : except for the d_{E_g} - and f -states that have approximately the same energies and are therefore indiscernible when plotted (inset of Fig. 2b). Note that the labels $d_{T_{2g}}$ and d_{E_g} are d -states with T_{2g} and E_g symmetries respectively. The separation of states at large attractive V is a consequence of the superlight effect. We emphasize that at $\mathbf{P} = 0$, the degeneracy of the p -, $d_{T_{2g}}$ -, d_{E_g} -, and f -states is three-fold, three-fold, two-fold and three-fold, respectively.

B. Binding Diagram

At zero pair momentum, we construct a phase diagram (Fig. 3) which shows where bound pairs form. States with nonzero angular momentum (i.e. p -, $d_{T_{2g}}$ -, d_{E_g} - and f -states) are insensitive to U , as evident in Fig. 3.

In comparison to other lattices with lower coordination numbers, pairs require stronger attractions for their

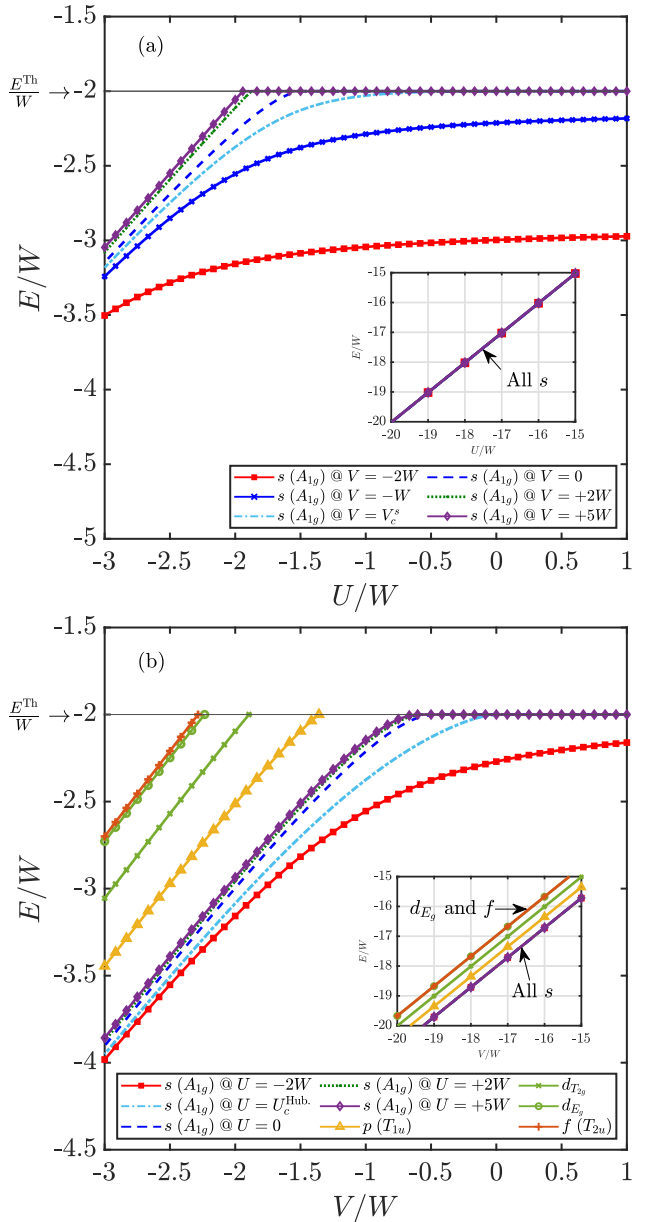


FIG. 2: The total energy of pairs for (a) the s -states only, and (b) all states of various symmetries. The critical attractions for the s -state are $U_c^{\text{Hub.}}(V=0) = -1.4874W$ and $V_c^s(U=0) = -0.4836W$. All states except the s -state are unaffected by U . The excited states (p , $d_{T_{2g}}$, d_{E_g} and f) only appear at strongly attractive V . At very large attractions U and V , all s -states have similar values (insets of panels (a) and (b)). For large intersite attraction, $V \rightarrow -\infty$, the d_{E_g} and f states have approximately the same energies and are indiscernible: inset of panel (b).

formation in the FCC lattice. This is due to the increase in kinetic energy with coordination number. The critical U or V required for binding can be found analytically

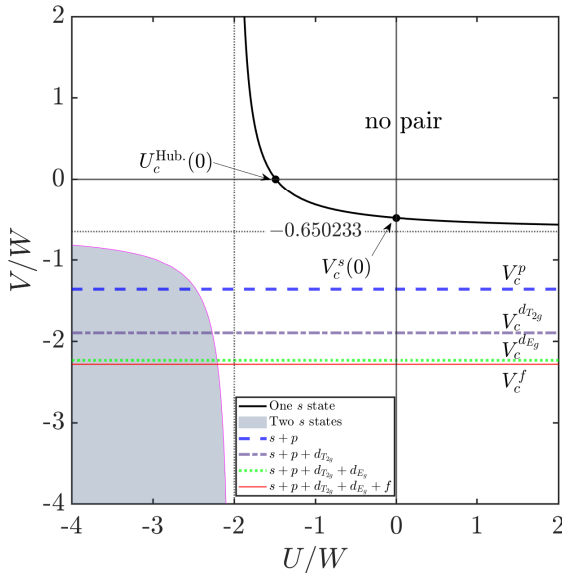


FIG. 3: [Color online] Binding diagram showing pair formation at $\mathbf{P} = 0$ in an FCC lattice. The top (black) curved line is the boundary that separates bound from unbound s -symmetry pairs, the (gray) shaded region enclosed by the (magenta) solid line indicates a region with two s -states, the (blue) thick dashed line represents the onset of triply degenerate p -states, the (purple) dash-dotted line shows the binding of a triple degenerate d -symmetry pair of T_{2g} symmetry (labeled $d_{T_{2g}}$), the (green) dotted line is the line below which two d -wave pairs with E_g symmetry start to form (labeled d_{E_g}) and the (red) solid line indicates the formation of a triply-degenerate f pairs. An s -state is guaranteed to form for attractions equal to or stronger than $U = -2W$, $V = -0.65023W$.

(refer to Appendix A for more details) via

$$V_c^s(U) \leq \frac{UL_0 - 1}{UL_0\mathcal{C} - \mathcal{C} - 12UL_1^2} \quad (14)$$

where $L_0 = -\sqrt{3}K_0^2/(8\pi^2t)$, $L_1 = 1/(24t) + L_0$, $\mathcal{C} = 12L_0 + 1/(2t)$ and $K_0 = K\left(\frac{\sqrt{3}-1}{2\sqrt{2}}\right) = 1.598142\dots$ is the complete elliptic integral of the first kind. Note that Eqn. (14) only holds when $\mathbf{P} = 0$.

The required potential to create bound onsite pairs with no intersite interaction is $U_c^{\text{Hub.}}(V=0) \approx -1.4874W$ (the negative Hubbard model, $V=0$). This is a slightly greater attraction relative to the simple cubic [9] and body-centered cubic [10] lattices. Equation (14) also yields the critical attraction $V_c^s(U=0) \approx -0.4836W$. At infinite intersite repulsion, the onsite s -state is guaranteed to form if $U_c^{\text{Hub.}}(V \rightarrow +\infty) \leq -2W$. Also, $V_c^s(+\infty) = -0.6502W$. The non- s pairs have critical intersite binding strength $V_c^p \approx -1.3586W$, $V_c^{d_{T_{2g}}} \approx -1.8945W$, $V_c^{d_{E_g}} \approx -2.2342W$, $V_c^f \approx -2.2847W$.

If measured in terms of their respective bandwidths, there are similarities in the critical attractions needed to

Pairing symmetry	Binding parameter	Minimum attraction required		
		SC	BCC	FCC
s -wave	$U(V=0)$	-1.3189 W_S	-1.4355 W_B	-1.4874 W_F
	$U(V=+\infty)$	-2 W_S	-2 W_B	-2 W_F
	$V(U=0)$	-0.6455 W_S	-0.6358 W_B	-0.4836 W_F
	$V(U=+\infty)$	-0.9789 W_S	-0.8858 W_B	-0.6502 W_F
p -wave (A_{2u})	V	-1.5885 W_S	-1.5828 W_B	-1.3586 W_F
d -wave (T_{2g})	V		-1.8804 W_B	-1.8945 W_F
d -wave (E_g)	V		-1.8034 W_S	-2.2342 W_F
f -wave (T_{2u})	V		-1.9639 W_B	-2.2847 W_F

TABLE I: Comparing critical binding strengths at $\mathbf{P} = 0$ in 3D cubic lattices (simple cubic, body-centered cubic, face-centered cubic). $W_S = 6t$, $W_B = 8t$, and $W_F = 12t$ are the respective half-bandwidths. We note that there are more pairing states in the FCC lattice than the other lattices.

bind two fermions in the simple cubic, BCC and FCC lattices. The summary of this comparison is given in Table I.

C. Dispersion

The pair energy at non-zero momentum is needed to estimate the pair mass. The dispersion of singlet and triplet states across the FCC Brillouin zone (BZ) for $U=+5W$ (repulsive) and $V=-2.3W$ (attractive) is shown in Fig. 4. To observe the dispersion of the excited states (d_{E_g} and f), an intersite interaction stronger than the bandwidth ($-2W$) is required (evident from Table I). Away from the Γ point, degeneracies are lifted and there are mixing and crossing of states, making it difficult to specify pair symmetries. However, our method guarantees unambiguous classification of singlets and triplets. The overall form of the dispersions has been confirmed at strong coupling with perturbation theory calculations (see Appendix B).

D. Pair Mass

The effective mass is calculated from the second derivative of the pair energy dispersion as

$$[m_i^*]^{-1} = \frac{1}{\hbar^2} \frac{\partial^2 E}{\partial P_i^2} \quad , \quad (15)$$

and masses can be seen in Fig. 5.

In some lattices (e.g. rectangular ladder [2], simple cubic [9], and BCC [10]), a superlight itinerant state is formed only when U and V are nearly equal and are both attractive which enhances the mobility of the pair via a single hop. However, for superlight pairs in staggered ladder [1] and triangular lattices [3], attractive onsite attraction is not required: a condition which is closer to physical systems which typically have onsite repulsion. The FCC lattice, due to its structure, is special and belongs to the latter group.

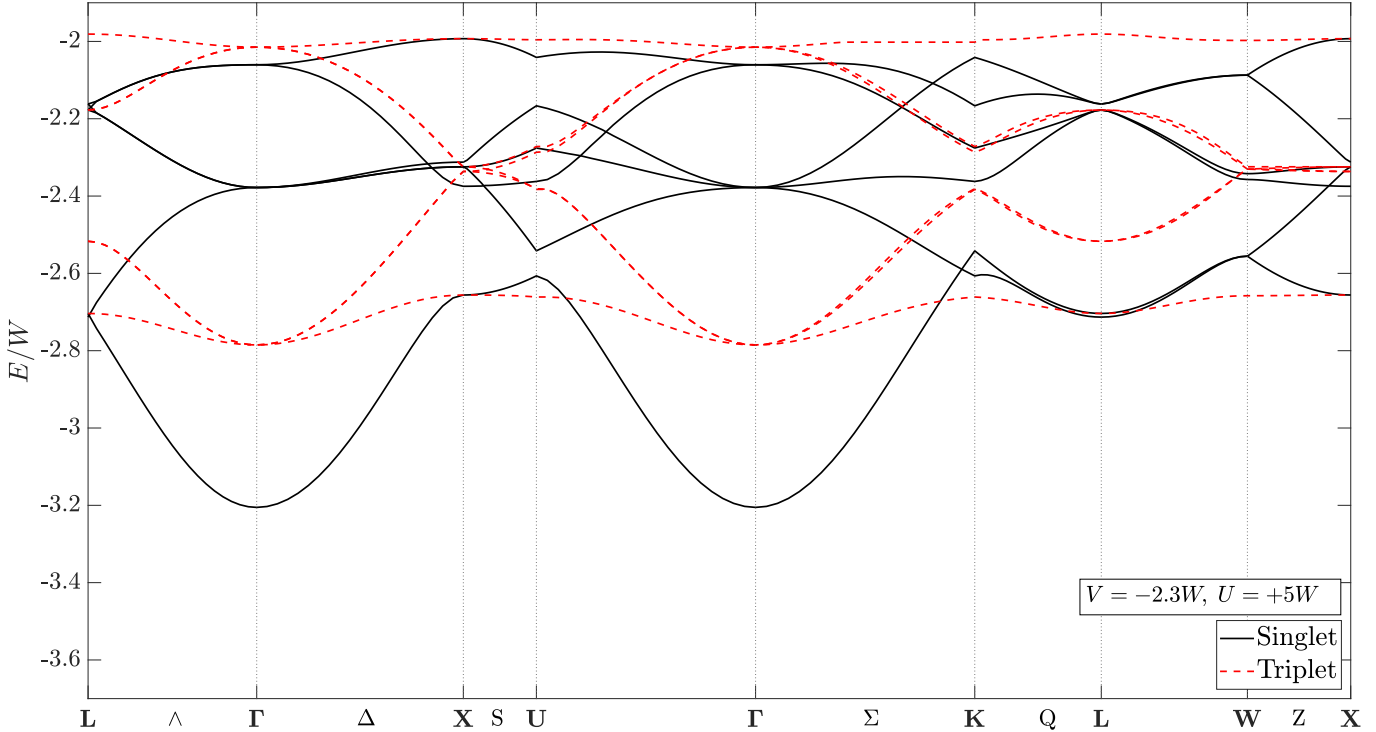


FIG. 4: Dispersion curve of bound pairs at $U = +5W$ and $V = -2.3W$. Moving away from the Γ point, degeneracies are lifted. Spin triplets are identified with a dashed (red) curve and spin singlets with solid (black) curve.

In the limit where the intersite interaction is attractive and dominant $V \rightarrow -\infty$, the pair mass does not increase infinitely (Fig. 5b) but is only *six times* heavier than a single particle's (i.e. $m^* = 6m_0$, see Appendix B for the full derivation). This result shows the *superlight* nature of pairs in the FCC lattice because the energy and the movement of the pair only linearly depend on t . Similar *low-mass* states were reported in lower dimensions (Refs. 2 and 3) at very strong attractive V . Superlight pair movement is depicted in Fig. 1.

On the other hand, in the limit where the onsite attraction is largely dominant $U \rightarrow -\infty$ and V is small or repulsive, the mass of the bound pair increases infinitely. In this case, the pair movement has a second-order effect in the hopping parameter t .

E. Pair Radius

The effective radius is obtained from the expression

$$\langle r^* \rangle = \sqrt{\frac{\sum_{\mathbf{n}} \mathbf{n}^2 \Psi^*(\mathbf{n}_1, \mathbf{n}_2) \Psi(\mathbf{n}_1, \mathbf{n}_2)}{\sum_{\mathbf{n}} \Psi^*(\mathbf{n}_1, \mathbf{n}_2) \Psi(\mathbf{n}_1, \mathbf{n}_2)}} , \quad (16)$$

where $\mathbf{n} = |\mathbf{n}_1 - \mathbf{n}_2|$. The radius is plotted in Fig. 6.

The size of the pair diverges near the threshold energy ($E \rightarrow E^{\text{Th}}$). This is because the pair is weakly bound and the pair wave function spreads over a distant lattice sites. If the particles unbind, the size becomes infinite.

When V is strongly attractive and dominates over U , we see the formation of a local intersite pair. A bound pair is local if its size is on the order of the lattice parameter. In contrast, if the Hubbard attraction is very strong and dominant, an onsite pair is formed.

F. Bose-Einstein Condensation

In this section, we examine if superlight pairs in an FCC lattice could Bose-condense at significant transition temperatures in the dilute limit. At low temperatures when pairs are well-separated and weakly-interacting, they can collectively form a condensate. The transition temperature is obtained from the Bose integral:

$$\frac{n_b}{\Omega_{\text{site}}} = \int \frac{d^3 \mathbf{P}}{(2\pi)^3} \frac{1}{\exp[(E_{\mathbf{P}} - E_0)/k_B T_{\text{BEC}}] - 1} \quad (17)$$

where $E_{\mathbf{P}}$ the pair dispersion.

The high energy tail of the Bose-Einstein distribution decreases rapidly, implying that only \mathbf{P} points where $E_{\mathbf{P}} - E_0 \lesssim k_B T_{\text{BEC}}$ contribute to the integral. This means that for pairs with a parabolic dispersion for $E_{\mathbf{P}} - E_0 \leq k_B T_{\text{BEC}}$, the transition temperature is given by the approximation:

$$T_{\text{BEC}} = \frac{3.31 \hbar^2}{m_b^* k_B} \left(\frac{n_b}{\Omega_{\text{site}}} \right)^{2/3} = \frac{3.31 \hbar^2}{\bar{m} m_0 k_B} \left(\frac{n_b}{\Omega_{\text{site}}} \right)^{2/3} \quad (18)$$

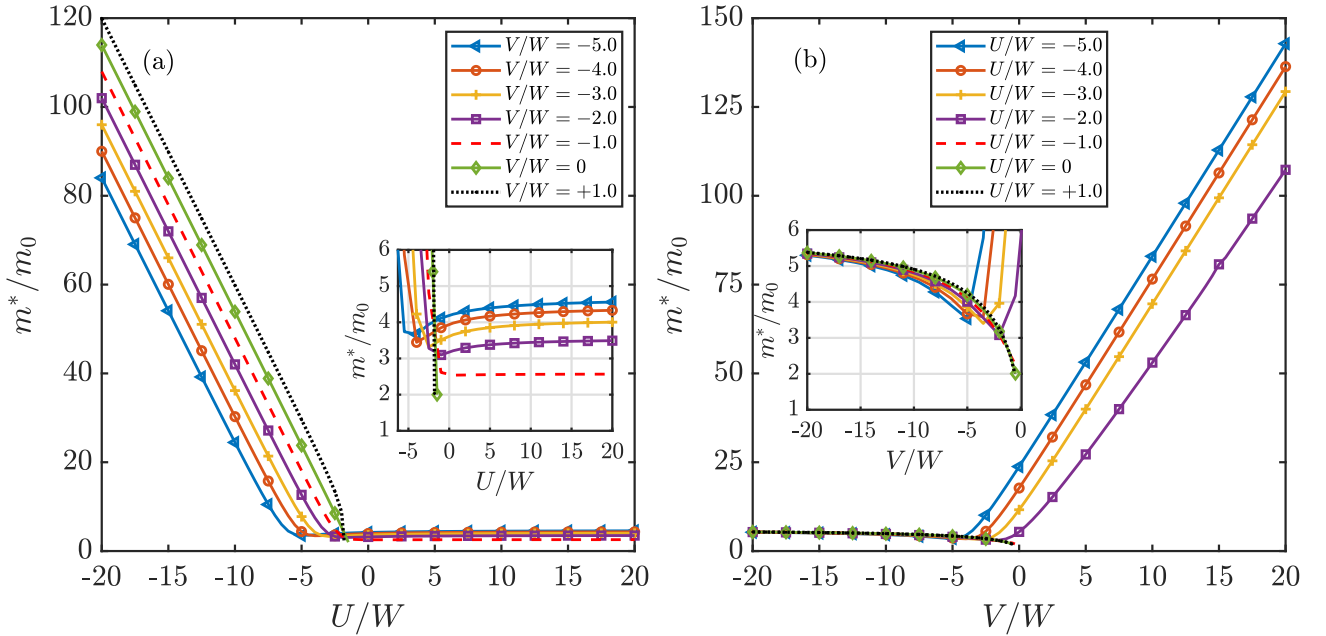


FIG. 5: [Color online] Dependence of the pair mass on (a) U , (b) V . A striking feature of a bound pair in the FCC lattice is its *superlight* nature. In the limit $V \rightarrow -\infty$, the pair mass does not increase infinitely but is only *six times* heavier than a single particle mass (inset of panel (b)). If compared with other 3D lattices, this is lighter by an order of magnitude.

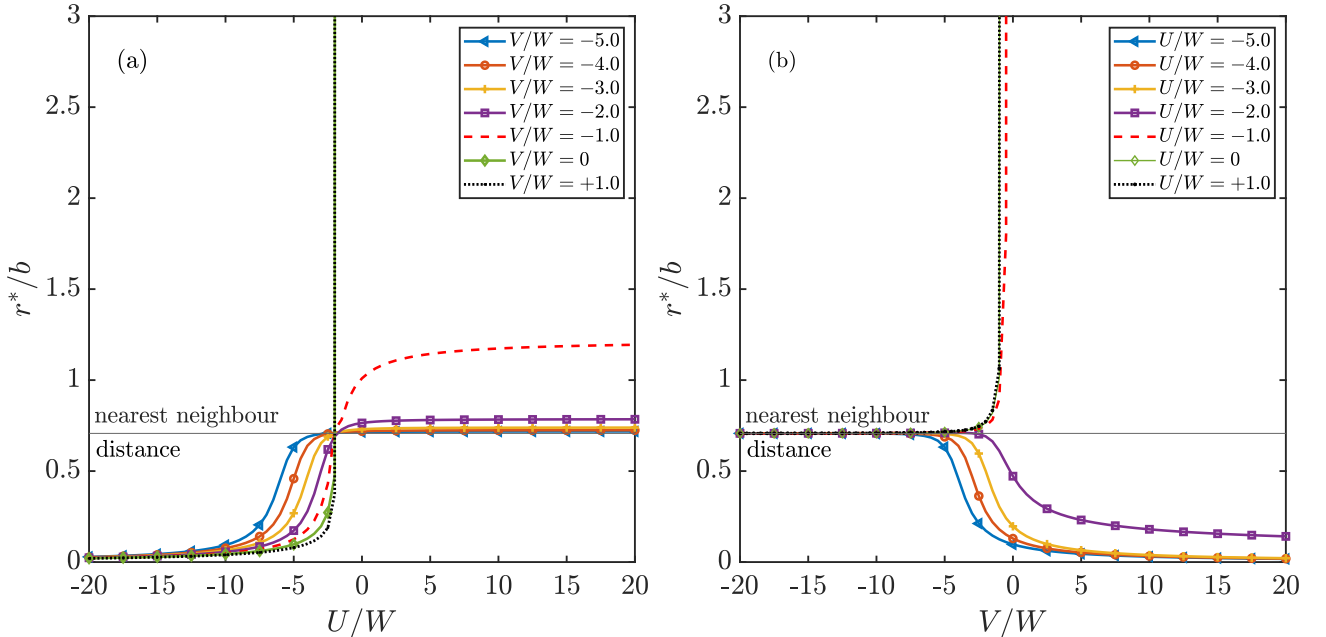


FIG. 6: [Color online] Radius in units of the lattice constant for (a) onsite interaction at different V , (b) intersite interaction for various U . The radius diverges at the binding threshold. Local pairs are formed when V is attractive and dominates, but when attractive Hubbard U dominates, the formation of an onsite pair is favored.

where m_b^* is the pair mass (m_0 is the mass of a free particle and the dimensionless mass $\bar{m} = m^*/m_0$), $\Omega_{\text{site}} = b^3/4$ is the volume of the Wigner–Seitz cell for the FCC lattice, and n_b is the number of pairs per lattice site. For our calculation, we use an exemplar lattice constant $b = 14.24\text{\AA}$ (consistent with the FCC fullerenes, although

we note that electrons are not dilute in fullerenes and further manipulations would be required to derive a UV model for such materials).

The transition temperatures for fixed n_b is plotted in Fig. 7. For condensation to take place, there must be pairs. This means that pairs must exist above T_{BEC} , i.e.

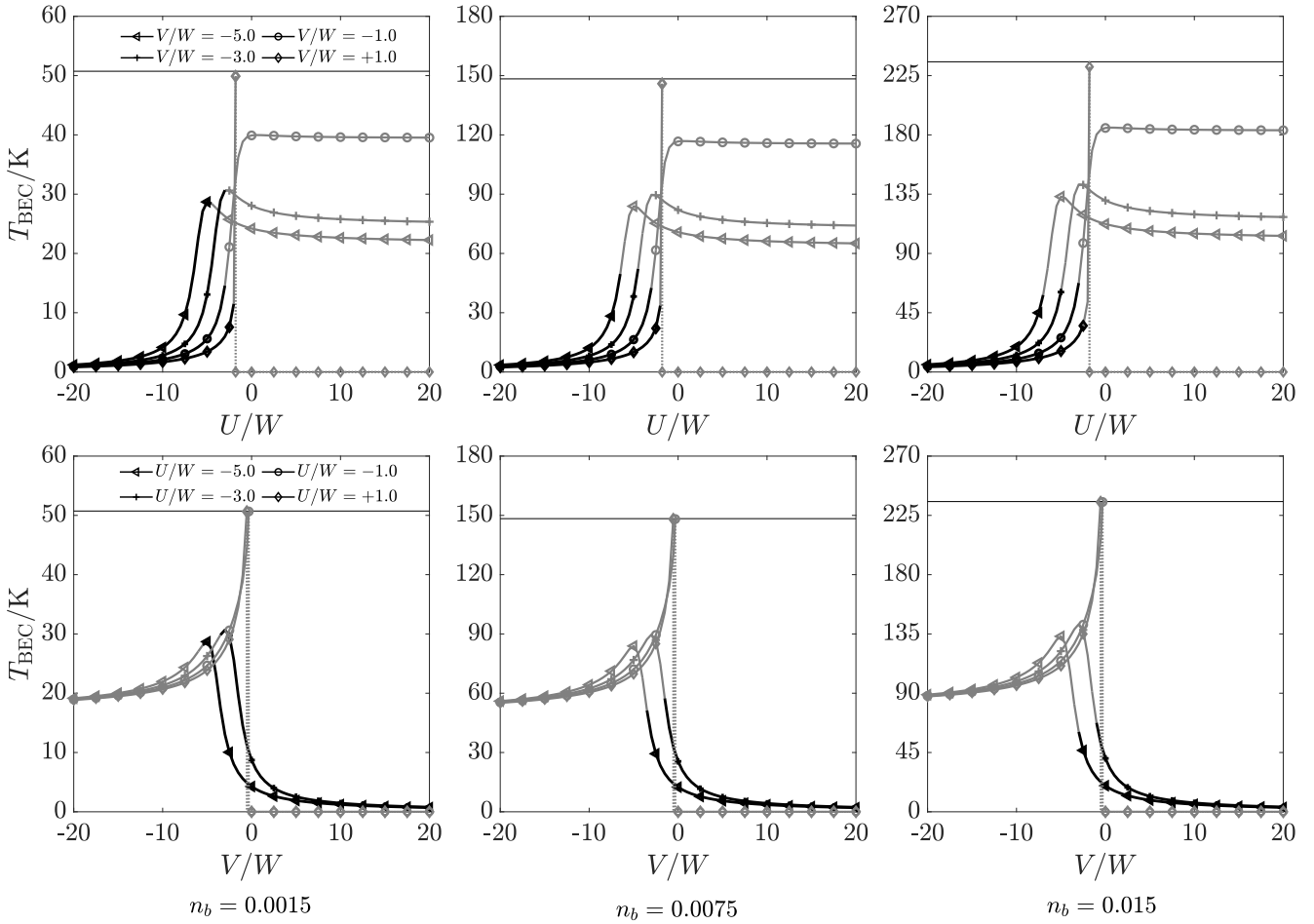


FIG. 7: Plots of BEC transition temperature for bound pairs in the dilute limit. The number of pairs per site n_b increases from left to right. Dark lines are used if n_b satisfies the pair overlap condition. We observe a flat region in T_{BEC} in the superlight regimes. The horizontal lines show T_{BEC} for pairs of mass $m^* = 2m_0$. The dotted regions (abrupt decrease to zero transition temperature) indicate $T_{\Delta} < T_{\text{BEC}}$ (so there are no preformed pairs).

$T_{\text{BEC}} < T_{\Delta}$, where $T_{\Delta} = \Delta/k_B$ is the pairing temperature and the binding energy is $\Delta = 2\varepsilon_0 - E_0$. The value $t = 0.04\text{eV}$ (which is consistent with fulleride superconductors [12]) is used to set the energy scale. The maximum n_b for which T_{BEC} is consistent with the effective mass approximation is estimated to be approximately 0.015. We require that pairs of radius $R' = \alpha r^*$ can fit into space without overlapping, i.e. that $n_b 16R'^3/3 < 1$. Assigning the value $\alpha = 5$ is suggested to minimize the overlap of wave functions of different pairs to about 1%. For the lowest n_b considered in this study, superlight pairs can yield a transition temperature up to 30 K (see Fig. 7 for $n_b = 0.0015$). When n_b is increased, the transition temperature goes up but these superlight pairs begin to overlap. Nonetheless, our calculation predicts a transition temperature up to 70 K when $n_b = 0.015$ that is consistent with the overlap condition stated above.

IV. DISCUSSION AND CONCLUSIONS

This paper explored the formation and the characteristic properties of fermion pairs in an FCC lattice. The consequences as to whether such pairs can Bose-condense in the dilute limit are also examined. We found superlight local pairs forming in the FCC lattice. When the inter-site attraction becomes infinitely large and U is repulsive, the pair mass is superlight; the bound pair is just six times heavier than a single particle mass. The FCC lattice is the 3D analogue of the triangular lattice and staggered ladder in this sense: intersite pairs formed on these lattices are superlight and can move freely via a single hop even in the strong coupling limit $V \rightarrow -\infty$. When conditions on overlap are maintained to keep pairs dilute and weakly interacting, the transition temperature is predicted to be as high as 70 K.

In conclusion, this work has shown that small intersite pairs formed in FCC lattice are an order of magnitude lighter than pairs in the simple cubic and body-centered cubic lattices. Consequentially, we propose that FCC

systems with a repulsive Hubbard U and moderate intersite attraction, V , would be a good place to search for high temperature superconductivity. We note that transition temperatures predicted here are similar to those

in FCC fulleride materials. While the fullerides are not dilute, it may be possible to determine an effective UV Hamiltonian with case of light doping away from half filling in such systems. We suggest this for future study.

[1] J. P. Hague, P. E. Kornilovitch, J. H. Samson, and A. S. Alexandrov, Superlight small bipolarons in the presence of a strong Coulomb repulsion, *Phys. Rev. Lett.* **98**, 037002 (2007).

[2] J. P. Hague, P. E. Kornilovitch, J. H. Samson, and A. S. Alexandrov, Superlight small bipolarons, *Journal of Physics: Condensed Matter* **19**, 255214 (2007).

[3] J. P. Hague, P. E. Kornilovitch, J. H. Samson, and A. S. Alexandrov, Singlet and triplet bipolarons on the triangular lattice, *Journal of Physics and Chemistry of Solids* **69**, 3304 (2008).

[4] J. P. Hague and P. E. Kornilovitch, Light and stable triplet bipolarons on square and triangular lattices, *Phys. Rev. B* **82**, 094301 (2010).

[5] J. E. Hirsch, Charge-density-wave to spin-density-wave transition in the extended Hubbard model, *Phys. Rev. Lett.* **53**, 2327 (1984).

[6] R. Micnas, J. Ranninger, and S. Robaszkiewicz, Superconductivity in narrow-band systems with local nonretarded attractive interactions, *Rev. Mod. Phys.* **62**, 113 (1990).

[7] P. Kornilovitch, Enhanced stability of bound pairs at nonzero lattice momenta, *Phys. Rev. B* **69**, 235110 (2004).

[8] M. Bak, Bound electron pairs on a triangular lattice in an extended Hubbard model, *Phys. Stat. Sol. B* **244**, 2421 (2007).

[9] A. R. Davenport, J. P. Hague, and P. E. Kornilovitch, Mobile small bipolarons on a three-dimensional cubic lattice, *Phys. Rev. B* **86**, 035106 (2012).

[10] G. D. Adebanjo, P. Kornilovitch, and J. Hague, Fermion pairing in body-centered-cubic quantum simulators of extended Hubbard models, arXiv preprint arXiv:2102.07744 (2021).

[11] O. Gunnarsson, Superconductivity in fullerides, *Rev. Mod. Phys.* **69**, 575 (1997).

[12] O. Gunnarsson, *Alkali-doped fullerides: narrow-band solids with unusual properties* (World Scientific, 2004).

[13] M. Capone, M. Fabrizio, C. Castellani, and E. Tosatti, Colloquium: Modeling the unconventional superconducting properties of expanded A_3C_{60} fullerides, *Rev. Mod. Phys.* **81**, 943 (2009).

[14] Y. Takada and T. Hotta, Superconductivity in the alkali-doped fullerides: competition of phonon-mediated attractions with Coulomb repulsions in polaron pairing, *International Journal of Modern Physics B* **12**, 3042 (1998).

[15] T. Morita, Use of a recurrence formula in computing the lattice Green function, *Journal of Physics A: Mathematical and General* **8**, 478 (1975).

[16] J. Cornwell, Appendix C - Character Tables for the Crystallographic Point Groups, in *Group Theory in Physics: An Introduction*, Techniques of Physics, Vol. 1 (Academic Press, San Diego, 1997) pp. 299 – 318.

[17] The normalization factors have been omitted.

[18] The subscript s is now used twice: $\hat{\Phi}_s$ means all possible singlet states (s,d,d^*) while Φ_s means an s -state only.

[19] M. L. Glasser and J. Boersma, Exact values for the cubic lattice Green functions, *Journal of Physics A: Mathematical and General* **33**, 5017 (2000).

Appendix A: UV model on face-centered cubic lattice

1. Schrödinger equation

The (anti-)symmetrized Schrödinger equation can be written as,

$$(E - \varepsilon_{\mathbf{k}_1} - \varepsilon_{\mathbf{k}_2})\phi_{\mathbf{k}_1 \mathbf{k}_2}^{\pm} = \frac{1}{N} \sum'_{\mathbf{q} \mathbf{a}_{\pm}} \hat{V}_{\mathbf{a}_{\pm}} \left\{ e^{i(\mathbf{q}-\mathbf{k}_1) \cdot \mathbf{a}_{\pm}} \pm e^{i(\mathbf{q}-\mathbf{k}_2) \cdot \mathbf{a}_{\pm}} \right\} \phi_{\mathbf{q}, \mathbf{k}_1 + \mathbf{k}_2 - \mathbf{q}}^{\pm} \quad (A1)$$

The prime in the summation means that a factor of $\frac{1}{2}$ must be included for the case $\mathbf{a}_+ = 0$. Spin singlets have solutions belonging to the symmetrized Schrödinger equation while spin triplets can be found from the anti-symmetrized version of Eqn. (A1).

We define the vectors for the singlets and triplets respectively as

$$\{\mathbf{a}_+\} = \{\mathbf{a}_0^+, \mathbf{a}_1^+, \mathbf{a}_2^+, \mathbf{a}_3^+, \mathbf{a}_4^+, \mathbf{a}_5^+, \mathbf{a}_6^+\} = \{(0, 0, 0), (\frac{1}{2}, \frac{1}{2}, 0), (0, \frac{1}{2}, \frac{1}{2}), (\frac{1}{2}, 0, \frac{1}{2}), (\frac{1}{2}, -\frac{1}{2}, 0), (0, \frac{1}{2}, -\frac{1}{2}), (-\frac{1}{2}, 0, \frac{1}{2})\}$$

$$\{\mathbf{a}_-\} = \{\mathbf{a}_1^-, \mathbf{a}_2^-, \mathbf{a}_3^-, \mathbf{a}_4^-, \mathbf{a}_5^-, \mathbf{a}_6^-\} = \{(\frac{1}{2}, \frac{1}{2}, 0), (0, \frac{1}{2}, \frac{1}{2}), (\frac{1}{2}, 0, \frac{1}{2}), (\frac{1}{2}, -\frac{1}{2}, 0), (0, \frac{1}{2}, -\frac{1}{2}), (-\frac{1}{2}, 0, \frac{1}{2})\}.$$

In this section, we set $b = 1$.

a. Symmetrized Schrödinger equation

Using the vectors $\{\mathbf{a}_+\}$ in Eqn. (A1), we obtain

$$\begin{aligned}
 (E - \varepsilon_{\mathbf{k}_1} - \varepsilon_{\mathbf{k}_2})\phi_{\mathbf{k}_1 \mathbf{k}_2}^+ &= \frac{1}{N} \sum_{\mathbf{q}} \left[\frac{1}{2} U(e^{i(\mathbf{q}-\mathbf{k}_1)\mathbf{a}_0^+} + e^{i(\mathbf{q}-\mathbf{k}_2)\mathbf{a}_0^+}) + V(e^{i(\mathbf{q}-\mathbf{k}_1)\mathbf{a}_1^+} + e^{i(\mathbf{q}-\mathbf{k}_2)\mathbf{a}_1^+}) \right. \\
 &+ V(e^{i(\mathbf{q}-\mathbf{k}_1)\mathbf{a}_2^+} + e^{i(\mathbf{q}-\mathbf{k}_2)\mathbf{a}_2^+}) + V(e^{i(\mathbf{q}-\mathbf{k}_1)\mathbf{a}_3^+} + e^{i(\mathbf{q}-\mathbf{k}_2)\mathbf{a}_3^+}) + V(e^{i(\mathbf{q}-\mathbf{k}_1)\mathbf{a}_4^+} + e^{i(\mathbf{q}-\mathbf{k}_2)\mathbf{a}_4^+}) \\
 &\left. + V(e^{i(\mathbf{q}-\mathbf{k}_1)\mathbf{a}_5^+} + e^{i(\mathbf{q}-\mathbf{k}_2)\mathbf{a}_5^+}) + V(e^{i(\mathbf{q}-\mathbf{k}_1)\mathbf{a}_6^+} + e^{i(\mathbf{q}-\mathbf{k}_2)\mathbf{a}_6^+}) \right] \phi_{\mathbf{q}, \mathbf{k}_1 + \mathbf{k}_2 - \mathbf{q}}^+ \\
 &= \frac{1}{N} \sum_{\mathbf{q}} \left[U + V e^{i(\frac{q_x}{2} + \frac{q_y}{2})} (e^{-i\mathbf{k}_1 \mathbf{a}_1^+} + e^{-i\mathbf{k}_2 \mathbf{a}_1^+}) + V e^{i(\frac{q_y}{2} + \frac{q_z}{2})} (e^{-i\mathbf{k}_1 \mathbf{a}_2^+} + e^{-i\mathbf{k}_2 \mathbf{a}_2^+}) + V e^{i(\frac{q_x}{2} + \frac{q_z}{2})} (e^{-i\mathbf{k}_1 \mathbf{a}_3^+} + e^{-i\mathbf{k}_2 \mathbf{a}_3^+}) \right. \\
 &\left. + V e^{i(\frac{q_x}{2} - \frac{q_y}{2})} (e^{-i\mathbf{k}_1 \mathbf{a}_4^+} + e^{-i\mathbf{k}_2 \mathbf{a}_4^+}) + V e^{i(\frac{q_y}{2} - \frac{q_z}{2})} (e^{-i\mathbf{k}_1 \mathbf{a}_5^+} + e^{-i\mathbf{k}_2 \mathbf{a}_5^+}) + V e^{i(-\frac{q_x}{2} + \frac{q_z}{2})} (e^{-i\mathbf{k}_1 \mathbf{a}_6^+} + e^{-i\mathbf{k}_2 \mathbf{a}_6^+}) \right] \phi_{\mathbf{q}, \mathbf{k}_1 + \mathbf{k}_2 - \mathbf{q}}^+ \quad (A2)
 \end{aligned}$$

The following basis functions can be used:

$$\begin{aligned}
 \Phi_0^+(\mathbf{P}) &= \frac{1}{N} \sum_{\mathbf{q}} \phi_{\mathbf{q}, \mathbf{P} - \mathbf{q}}^+, \quad \Phi_1^+(\mathbf{P}) = \frac{1}{N} \sum_{\mathbf{q}} e^{i(\frac{q_x}{2} + \frac{q_y}{2})} \phi_{\mathbf{q}, \mathbf{P} - \mathbf{q}}^+, \quad \Phi_2^+(\mathbf{P}) = \frac{1}{N} \sum_{\mathbf{q}} e^{i(\frac{q_y}{2} + \frac{q_z}{2})} \phi_{\mathbf{q}, \mathbf{P} - \mathbf{q}}^+ \\
 \Phi_3^+(\mathbf{P}) &= \frac{1}{N} \sum_{\mathbf{q}} e^{i(\frac{q_x}{2} + \frac{q_z}{2})} \phi_{\mathbf{q}, \mathbf{P} - \mathbf{q}}^+, \quad \Phi_4^+(\mathbf{P}) = \frac{1}{N} \sum_{\mathbf{q}} e^{i(\frac{q_x}{2} - \frac{q_y}{2})} \phi_{\mathbf{q}, \mathbf{P} - \mathbf{q}}^+ \\
 \Phi_5^+(\mathbf{P}) &= \frac{1}{N} \sum_{\mathbf{q}} e^{i(\frac{q_y}{2} - \frac{q_z}{2})} \phi_{\mathbf{q}, \mathbf{P} - \mathbf{q}}^+, \quad \Phi_6^+(\mathbf{P}) = \frac{1}{N} \sum_{\mathbf{q}} e^{i(-\frac{q_x}{2} + \frac{q_z}{2})} \phi_{\mathbf{q}, \mathbf{P} - \mathbf{q}}^+ \quad (A3)
 \end{aligned}$$

where $\mathbf{P} = \mathbf{k}_1 + \mathbf{k}_2$. The wave function in Eqn. (A2) expressed in terms of the basis functions Eqn. (A3) is

$$\begin{aligned}
 \phi_{\mathbf{k}_1 \mathbf{k}_2}^+ &= \frac{1}{(E - \varepsilon_{\mathbf{k}_1} - \varepsilon_{\mathbf{k}_2})} \left\{ U \Phi_0^+(\mathbf{P}) + V \Phi_1^+(\mathbf{P}) (e^{-i\mathbf{k}_1 \mathbf{a}_1^+} + e^{-i\mathbf{k}_2 \mathbf{a}_1^+}) + V \Phi_2^+(\mathbf{P}) (e^{-i\mathbf{k}_1 \mathbf{a}_2^+} + e^{-i\mathbf{k}_2 \mathbf{a}_2^+}) \right. \\
 &+ V \Phi_3^+(\mathbf{P}) (e^{-i\mathbf{k}_1 \mathbf{a}_3^+} + e^{-i\mathbf{k}_2 \mathbf{a}_3^+}) + V \Phi_4^+(\mathbf{P}) (e^{-i\mathbf{k}_1 \mathbf{a}_4^+} + e^{-i\mathbf{k}_2 \mathbf{a}_4^+}) + V \Phi_5^+(\mathbf{P}) (e^{-i\mathbf{k}_1 \mathbf{a}_5^+} + e^{-i\mathbf{k}_2 \mathbf{a}_5^+}) \\
 &\left. + V \Phi_6^+(\mathbf{P}) (e^{-i\mathbf{k}_1 \mathbf{a}_6^+} + e^{-i\mathbf{k}_2 \mathbf{a}_6^+}) \right\} \quad (A4)
 \end{aligned}$$

Substituting Eqn. (A4) into each entry of Eqn. (A3) and redefining $q_j = q'_j + \frac{P_j}{2}$ leads to seven self-consistent equations. The first is

$$\begin{aligned}
 \tilde{\Phi}_0^+(\mathbf{P}) &= U L_{000}(\mathbf{P}) \tilde{\Phi}_0^+(\mathbf{P}) + V \left[L_{110}(\mathbf{P}) + L_{\bar{1}\bar{1}0}(\mathbf{P}) \right] \tilde{\Phi}_1^+(\mathbf{P}) + V \left[L_{011}(\mathbf{P}) + L_{0\bar{1}\bar{1}}(\mathbf{P}) \right] \tilde{\Phi}_2^+(\mathbf{P}) \\
 &+ V \left[L_{101}(\mathbf{P}) + L_{\bar{1}0\bar{1}}(\mathbf{P}) \right] \tilde{\Phi}_3^+(\mathbf{P}) + V \left[L_{1\bar{1}0}(\mathbf{P}) + L_{\bar{1}10}(\mathbf{P}) \right] \tilde{\Phi}_4^+(\mathbf{P}) \\
 &+ V \left[L_{01\bar{1}}(\mathbf{P}) + L_{0\bar{1}\bar{1}}(\mathbf{P}) \right] \tilde{\Phi}_5^+(\mathbf{P}) + V \left[L_{\bar{1}01}(\mathbf{P}) + L_{10\bar{1}}(\mathbf{P}) \right] \tilde{\Phi}_6^+(\mathbf{P}) \quad (A5)
 \end{aligned}$$

where $\tilde{\Phi}_i^+(\mathbf{P}) = e^{\frac{-i}{2}(\mathbf{P} \cdot \mathbf{a}_i^+)} \Phi_i^+$ (where $i = 0, 1, \dots, 6$), have phase factors which provides information about the center-of-mass motion of the bound state. Furthermore, the L 's represent the Green's functions of the FCC lattice which are defined as

$$L_{lmn}(\mathbf{P}) = \frac{1}{N} \sum_{\mathbf{q}'} \frac{e^{i(l\frac{q'_x}{2} + m\frac{q'_y}{2} + n\frac{q'_z}{2})}}{E - \varepsilon_{\frac{\mathbf{P}}{2} + \mathbf{q}'} - \varepsilon_{\frac{\mathbf{P}}{2} - \mathbf{q}'}} = - \int_{-2\pi}^{2\pi} \int_{-2\pi}^{2\pi} \int_{-2\pi}^{2\pi} \frac{dq'_x dq'_y dq'_z}{(4\pi)^3} \frac{\cos(l\frac{q'_x}{2} + m\frac{q'_y}{2} + n\frac{q'_z}{2})}{|E| + \varepsilon_{\frac{\mathbf{P}}{2} + \mathbf{q}'} + \varepsilon_{\frac{\mathbf{P}}{2} - \mathbf{q}'}} \quad (A6)$$

Instead of writing a negative subscript along a coordinate, we place a bar above it to keep notation compact. For the present problem where interactions are only limited to nearest-neighbor distances, l, m and n take the values 0, ± 1 , and ± 2 .

Combining all seven independent self-consistent equations for all spin-singlets at arbitrary momentum gives

$$\begin{pmatrix} UL_{000} & V[L_{110} + L_{\bar{1}\bar{1}0}] & V[L_{011} + L_{\bar{0}\bar{1}\bar{1}}] & V[L_{101} + L_{\bar{1}0\bar{1}}] & V[L_{1\bar{1}0} + L_{\bar{1}10}] & V(L_{01\bar{1}} + L_{0\bar{1}\bar{1}}) & V[L_{\bar{1}01} + L_{10\bar{1}}] \\ UL_{110} & V[L_{000} + L_{220}] & V[L_{10\bar{1}} + L_{12\bar{1}}] & V[L_{01\bar{1}} + L_{21\bar{1}}] & V[L_{020} + L_{200}] & V[L_{101} + L_{12\bar{1}}] & V[L_{21\bar{1}} + L_{011}] \\ UL_{011} & V[L_{\bar{1}01} + L_{12\bar{1}}] & V[L_{000} + L_{022}] & V[L_{\bar{1}10} + L_{11\bar{2}}] & V[L_{\bar{1}21} + L_{10\bar{1}}] & V[L_{002} + L_{020}] & V[L_{110} + L_{\bar{1}12}] \\ UL_{101} & V[L_{0\bar{1}\bar{1}} + L_{21\bar{1}}] & V[L_{\bar{1}\bar{1}0} + L_{11\bar{2}}] & V[L_{000} + L_{202}] & V[L_{011} + L_{2\bar{1}\bar{1}}] & V[L_{1\bar{1}2} + L_{110}] & V[L_{200} + L_{002}] \\ UL_{\bar{1}10} & V[L_{0\bar{2}0} + L_{200}] & V[L_{1\bar{2}\bar{1}} + L_{101}] & V[L_{0\bar{1}\bar{1}} + L_{2\bar{1}\bar{1}}] & V[L_{000} + L_{2\bar{2}0}] & V[L_{1\bar{2}\bar{1}} + L_{10\bar{1}}] & V[L_{2\bar{1}\bar{1}} + L_{0\bar{1}1}] \\ UL_{01\bar{1}} & V[L_{10\bar{1}} + L_{12\bar{1}}] & V[L_{002} + L_{020}] & V[L_{11\bar{2}} + L_{110}] & V[L_{12\bar{1}} + L_{10\bar{1}}] & V[L_{000} + L_{02\bar{2}}] & V[L_{11\bar{2}} + L_{110}] \\ UL_{\bar{1}01} & V[L_{\bar{2}\bar{1}\bar{1}} + L_{011}] & V[L_{\bar{1}\bar{1}0} + L_{\bar{1}\bar{1}2}] & V[L_{\bar{2}00} + L_{002}] & V[L_{\bar{2}11} + L_{0\bar{1}1}] & V[L_{\bar{1}\bar{1}2} + L_{\bar{1}10}] & V[L_{000} + L_{\bar{2}02}] \end{pmatrix} \begin{pmatrix} \tilde{\Phi}_0^+ \\ \tilde{\Phi}_1^+ \\ \tilde{\Phi}_2^+ \\ \tilde{\Phi}_3^+ \\ \tilde{\Phi}_4^+ \\ \tilde{\Phi}_5^+ \\ \tilde{\Phi}_6^+ \end{pmatrix} = \begin{pmatrix} \tilde{\Phi}_0^+ \\ \tilde{\Phi}_1^+ \\ \tilde{\Phi}_2^+ \\ \tilde{\Phi}_3^+ \\ \tilde{\Phi}_4^+ \\ \tilde{\Phi}_5^+ \\ \tilde{\Phi}_6^+ \end{pmatrix} \quad (A7)$$

b. Anti-symmetrized Schrödinger equation

The anti-symmetrized equation is found by substituting $\{\mathbf{a}_-\}$ in Eqn. (A1),

$$\begin{aligned} (E - \varepsilon_{\mathbf{k}_1} - \varepsilon_{\mathbf{k}_2})\phi_{\mathbf{k}_1 \mathbf{k}_2}^- = & \frac{1}{N} \sum_{\mathbf{q}} \left[V e^{i(\frac{q_x}{2} + \frac{q_y}{2})} (e^{-i\mathbf{k}_1 \mathbf{a}_1^-} - e^{-i\mathbf{k}_2 \mathbf{a}_1^-}) + V e^{i(\frac{q_y}{2} + \frac{q_z}{2})} (e^{-i\mathbf{k}_1 \mathbf{a}_2^-} - e^{-i\mathbf{k}_2 \mathbf{a}_2^-}) \right. \\ & + V e^{i(\frac{q_x}{2} + \frac{q_z}{2})} (e^{-i\mathbf{k}_1 \mathbf{a}_3^-} - e^{-i\mathbf{k}_2 \mathbf{a}_3^-}) + V e^{i(\frac{q_x}{2} - \frac{q_y}{2})} (e^{-i\mathbf{k}_1 \mathbf{a}_4^-} - e^{-i\mathbf{k}_2 \mathbf{a}_4^-}) \\ & \left. + V e^{i(\frac{q_y}{2} - \frac{q_z}{2})} (e^{-i\mathbf{k}_1 \mathbf{a}_5^-} - e^{-i\mathbf{k}_2 \mathbf{a}_5^-}) + V e^{i(-\frac{q_x}{2} + \frac{q_z}{2})} (e^{-i\mathbf{k}_1 \mathbf{a}_6^-} - e^{-i\mathbf{k}_2 \mathbf{a}_6^-}) \right] \phi_{\mathbf{q}, \mathbf{k}_1 + \mathbf{k}_2 - \mathbf{q}}^- \end{aligned} \quad (A8)$$

Similar basis functions can be used to the singlet case:

$$\begin{aligned} \Phi_1^-(\mathbf{P}) &= \frac{1}{N} \sum_{\mathbf{q}} e^{i(\frac{q_x}{2} + \frac{q_y}{2})} \phi_{\mathbf{q}, \mathbf{P} - \mathbf{q}}^-, \quad \Phi_2^-(\mathbf{P}) = \frac{1}{N} \sum_{\mathbf{q}} e^{i(\frac{q_y}{2} + \frac{q_z}{2})} \phi_{\mathbf{q}, \mathbf{P} - \mathbf{q}}^- \\ \Phi_3^-(\mathbf{P}) &= \frac{1}{N} \sum_{\mathbf{q}} e^{i(\frac{q_x}{2} + \frac{q_z}{2})} \phi_{\mathbf{q}, \mathbf{P} - \mathbf{q}}^-, \quad \Phi_4^-(\mathbf{P}) = \frac{1}{N} \sum_{\mathbf{q}} e^{i(\frac{q_x}{2} - \frac{q_y}{2})} \phi_{\mathbf{q}, \mathbf{P} - \mathbf{q}}^- \\ \Phi_5^-(\mathbf{P}) &= \frac{1}{N} \sum_{\mathbf{q}} e^{i(\frac{q_y}{2} - \frac{q_z}{2})} \phi_{\mathbf{q}, \mathbf{P} - \mathbf{q}}^-, \quad \Phi_6^-(\mathbf{P}) = \frac{1}{N} \sum_{\mathbf{q}} e^{i(-\frac{q_x}{2} + \frac{q_z}{2})} \phi_{\mathbf{q}, \mathbf{P} - \mathbf{q}}^- \end{aligned} \quad (A9)$$

leading to

$$\begin{aligned} \tilde{\Phi}_1^-(\mathbf{P}) &= V[L_{000} - L_{220}] \tilde{\Phi}_1^-(\mathbf{P}) + V[L_{10\bar{1}} - L_{12\bar{1}}] \tilde{\Phi}_2^-(\mathbf{P}) + V[L_{01\bar{1}} - L_{21\bar{1}}] \tilde{\Phi}_3^-(\mathbf{P}) + V[L_{020} - L_{200}] \tilde{\Phi}_4^-(\mathbf{P}) \\ &+ V[L_{101} - L_{12\bar{1}}] \tilde{\Phi}_5^-(\mathbf{P}) + V[L_{21\bar{1}} - L_{011}] \tilde{\Phi}_6^-(\mathbf{P}) \end{aligned} \quad (A10)$$

The combined self-consistent equations for all triplets are

$$\begin{pmatrix} V[L_{000} - L_{220}] & V[L_{10\bar{1}} - L_{12\bar{1}}] & V[L_{01\bar{1}} - L_{21\bar{1}}] & V[L_{020} - L_{200}] & V[L_{101} - L_{12\bar{1}}] & V[L_{21\bar{1}} - L_{011}] \\ V[L_{\bar{1}01} - L_{12\bar{1}}] & V[L_{000} - L_{022}] & V[L_{\bar{1}10} - L_{11\bar{2}}] & V[L_{\bar{1}21} - L_{101}] & V[L_{002} - L_{020}] & V[L_{110} - L_{\bar{1}12}] \\ V[L_{0\bar{1}\bar{1}} - L_{21\bar{1}}] & V[L_{\bar{1}\bar{1}0} - L_{11\bar{2}}] & V[L_{000} - L_{202}] & V[L_{011} - L_{2\bar{1}\bar{1}}] & V[L_{1\bar{1}2} - L_{110}] & V[L_{200} - L_{002}] \\ V[L_{0\bar{2}0} - L_{200}] & V[L_{1\bar{2}\bar{1}} - L_{101}] & V[L_{0\bar{1}\bar{1}} - L_{2\bar{1}\bar{1}}] & V[L_{000} - L_{2\bar{2}0}] & V[L_{1\bar{2}\bar{1}} - L_{10\bar{1}}] & V[L_{2\bar{1}\bar{1}} - L_{0\bar{1}1}] \\ V[L_{\bar{1}0\bar{1}} - L_{12\bar{1}}] & V[L_{002} - L_{020}] & V[L_{\bar{1}1\bar{2}} - L_{110}] & V[L_{\bar{1}2\bar{1}} - L_{10\bar{1}}] & V[L_{000} - L_{02\bar{2}}] & V[L_{11\bar{2}} - L_{\bar{1}10}] \\ V[L_{\bar{2}\bar{1}\bar{1}} - L_{011}] & V[L_{\bar{1}\bar{1}0} - L_{\bar{1}\bar{1}2}] & V[L_{\bar{2}00} - L_{002}] & V[L_{\bar{2}11} - L_{0\bar{1}1}] & V[L_{\bar{1}\bar{1}2} - L_{\bar{1}10}] & V[L_{000} - L_{\bar{2}02}] \end{pmatrix} \begin{pmatrix} \tilde{\Phi}_1^- \\ \tilde{\Phi}_2^- \\ \tilde{\Phi}_3^- \\ \tilde{\Phi}_4^- \\ \tilde{\Phi}_5^- \\ \tilde{\Phi}_6^- \end{pmatrix} = \begin{pmatrix} \tilde{\Phi}_1^- \\ \tilde{\Phi}_2^- \\ \tilde{\Phi}_3^- \\ \tilde{\Phi}_4^- \\ \tilde{\Phi}_5^- \\ \tilde{\Phi}_6^- \end{pmatrix} \quad (A11)$$

2. Pair energy for Γ point

At the Γ point,

$$\begin{aligned}
L_{lmn}(0) &= \frac{1}{N} \sum_{\mathbf{q}'} \frac{e^{i(l\frac{q'_x}{2} + m\frac{q'_y}{2} + n\frac{q'_z}{2})}}{E - 2\varepsilon_{\mathbf{q}'}} \\
&= - \int_{-2\pi}^{2\pi} \int_{-2\pi}^{2\pi} \int_{-2\pi}^{2\pi} \frac{dq'_x dq'_y dq'_z}{(4\pi)^3} \frac{\cos(l\frac{q'_x}{2}) \cos(m\frac{q'_y}{2}) \cos(n\frac{q'_z}{2})}{|E| - 8t \left\{ \cos(\frac{q'_x}{2}) \cos(\frac{q'_y}{2}) + \cos(\frac{q'_x}{2}) \cos(\frac{q'_z}{2}) + \cos(\frac{q'_y}{2}) \cos(\frac{q'_z}{2}) \right\}} \\
&= - \frac{1}{(2\pi)^3} \int_{-\pi}^{\pi} \int_{-\pi}^{\pi} \int_{-\pi}^{\pi} \frac{\cos(lq''_x) \cos(mq''_y) \cos(nq''_z)}{|E| - 8t \left\{ \cos(q''_x) \cos(q''_y) + \cos(q''_x) \cos(q''_z) + \cos(q''_y) \cos(q''_z) \right\}} dq''_x dq''_y dq''_z : \quad (q''_j = \frac{q'_j}{2}) \\
\end{aligned} \tag{A12}$$

Because some of the Green's functions are identical due to symmetry properties [15], we may then use the simplifications below

$$\begin{aligned}
L_{000} &= L_0 \\
L_{110} &= L_{101} = L_{011} = L_{\bar{1}01} = L_{0\bar{1}1} = L_{10\bar{1}} = L_{\bar{1}0\bar{1}} = L_{01\bar{1}} = L_{\bar{1}1\bar{1}} = L_{0\bar{1}\bar{1}} = L_{1\bar{1}0} = L_{\bar{1}\bar{1}0} \equiv L_1 \\
L_{220} &= L_{022} = L_{202} = L_{2\bar{2}0} = L_{0\bar{2}\bar{2}} = L_{\bar{2}02} \equiv L_2 \\
L_{200} &= L_{020} = L_{002} = L_{\bar{2}00} = L_{0\bar{2}\bar{0}} = L_{00\bar{2}} \equiv L_3 \\
L_{211} &= L_{121} = L_{112} = L_{\bar{2}11} = L_{1\bar{2}1} = L_{11\bar{2}} = L_{\bar{1}\bar{1}2} = \dots \equiv L_4
\end{aligned} \tag{A13}$$

to modify our dispersion matrices (A7) and (A11) to obtain (at the Γ point, $\tilde{\Phi}_i^{\pm} = \Phi_i^{\pm}$) :

$$\underbrace{\begin{pmatrix} UL_0 & 2VL_1 & 2VL_1 & 2VL_1 & 2VL_1 & 2VL_1 & 2VL_1 \\ UL_1 & V[L_0 + L_2] & V[L_1 + L_4] & V[L_1 + L_4] & 2VL_3 & V[L_1 + L_4] & V[L_4 + L_1] \\ UL_1 & V[L_1 + L_4] & V[L_0 + L_2] & V[L_1 + L_4] & V[L_4 + L_1] & 2VL_3 & V[L_1 + L_4] \\ UL_1 & V[L_1 + L_4] & V[L_1 + L_4] & V[L_0 + L_2] & V[L_1 + L_4] & V[L_4 + L_1] & 2VL_3 \\ UL_1 & 2VL_3 & V[L_4 + L_1] & V[L_1 + L_4] & V[L_0 + L_2] & V[L_4 + L_1] & V[L_4 + L_1] \\ UL_1 & V[L_1 + L_4] & 2VL_3 & V[L_4 + L_1] & V[L_4 + L_1] & V[L_0 + L_2] & V[L_4 + L_1] \\ UL_1 & V[L_4 + L_1] & V[L_1 + L_4] & 2VL_3 & V[L_4 + L_1] & V[L_4 + L_1] & V[L_0 + L_2] \end{pmatrix}}_{\hat{L}_{singlet}} = \underbrace{\begin{pmatrix} \Phi_0^+ \\ \Phi_1^+ \\ \Phi_2^+ \\ \Phi_3^+ \\ \Phi_4^+ \\ \Phi_5^+ \\ \Phi_6^+ \end{pmatrix}}_{\hat{\Phi}_{singlet}} \tag{A14}$$

$$\underbrace{\begin{pmatrix} V[L_0 - L_2] & V[L_1 - L_4] & V[L_1 - L_4] & 0 & V[L_1 - L_4] & V[L_4 - L_1] \\ V[L_1 - L_4] & V[L_0 - L_2] & V[L_1 - L_4] & V[L_4 - L_1] & 0 & V[L_1 - L_4] \\ V[L_1 - L_4] & V[L_1 - L_4] & V[L_0 - L_2] & V[L_1 - L_4] & V[L_4 - L_1] & 0 \\ 0 & V[L_4 - L_1] & V[L_1 - L_4] & V[L_0 - L_2] & V[L_4 - L_1] & V[L_4 - L_1] \\ V[L_1 - L_4] & 0 & V[L_4 - L_1] & V[L_4 - L_1] & V[L_0 - L_2] & V[L_4 - L_1] \\ V[L_4 - L_1] & V[L_1 - L_4] & 0 & V[L_4 - L_1] & V[L_4 - L_1] & V[L_0 - L_2] \end{pmatrix}}_{\hat{L}_{triplet}} = \underbrace{\begin{pmatrix} \Phi_1^- \\ \Phi_2^- \\ \Phi_3^- \\ \Phi_4^- \\ \Phi_5^- \\ \Phi_6^- \end{pmatrix}}_{\hat{\Phi}_{triplet}} \tag{A15}$$

We may rewrite the matrices above as

$$\hat{L}_{s,t} \hat{\Phi}_{s,t} = \lambda_{s,t} \hat{\Phi}_{s,t} \tag{A16}$$

to form an eigenvalue problem where \hat{L}_s and \hat{L}_t are the singlet and triplet dispersion matrices, λ_s and λ_t being the eigenvalues corresponding to singlet $\hat{\Phi}_s$ and triplet $\hat{\Phi}_t$ eigenvectors respectively. To find the pair energy, we select E , compute L and then λ . A true pair state corresponds to $\lambda = 1$. Thus, all pair energies can be found

by adjusting E and searching for $\lambda = 1$ using standard binary search algorithms.

As the Green's functions and dispersion matrices become more simplified at the Γ point of the FCC lattice, one can take further advantage of this high symmetry point. We use this point to evaluate the binding conditions for the formation of the bound states (with s -, p -, $d_{T_{2g}}$ -, d_{E_g} - and f - symmetries). Via the irreducible representations of the O_h group [16], we can determine

some linear combinations (excluding the normalization constants) of the eigenvector by performing the 48 operations on the FCC lattice. Note that the eigenfunction Φ_0^+ is at the center of zone and therefore remains unchanged due to the operations. These operations yield the irreducible representations for both the singlet and triplet states as

$$\begin{aligned}\Gamma_{\text{singlet}}^{\text{fcc}} &= A_{1g} \oplus E_g \oplus T_{2g} \\ \Gamma_{\text{triplet}}^{\text{fcc}} &= T_{1u} \oplus T_{2u}\end{aligned}\quad (\text{A17})$$

A_{1g} is s -symmetrical, E_g and T_{2g} are of d -symmetry, T_{1u} has p -symmetry whilst T_{2u} forms an f -symmetric state. An example of a symmetrized linear combinations for the singlets is

$$\chi^{A_{1g}} = \Phi_1^+ + \Phi_2^+ + \Phi_3^+ + \Phi_4^+ + \Phi_5^+ + \Phi_6^+ \quad (\text{A18})$$

$$\chi^{T_{2g}} = \begin{cases} \Phi_1^+ - \Phi_4^+ \\ \Phi_3^+ - \Phi_6^+ \\ \Phi_2^+ - \Phi_5^+ \end{cases} \quad (\text{A19})$$

$$\chi^{E_g} = \begin{cases} \Phi_1^+ - 2\Phi_2^+ + \Phi_3^+ + \Phi_4^+ - 2\Phi_5^+ + \Phi_6^+ \\ \Phi_1^+ - \Phi_3^+ + \Phi_4^+ - \Phi_6^+ \end{cases} \quad (\text{A20})$$

and for the triplets is

$$\chi^{T_{1u}} = \begin{cases} \Phi_1^- + \Phi_2^- - \Phi_4^- + \Phi_5^- \\ \Phi_1^- + \Phi_3^- + \Phi_4^- - \Phi_6^- \\ -\Phi_2^- - \Phi_3^- + \Phi_5^- - \Phi_6^- \end{cases} \quad (\text{A21})$$

$$\chi^{T_{2u}} = \begin{cases} \Phi_2^- - \Phi_3^- - \Phi_5^- - \Phi_6^- \\ \Phi_1^- - \Phi_3^- + \Phi_4^- + \Phi_6^- \\ \Phi_1^- - \Phi_2^- - \Phi_4^- - \Phi_5^- \end{cases} \quad (\text{A22})$$

Allowing transformation to a new orthogonal basis [17], [18]

$$\begin{pmatrix} \Phi_0 \\ \Phi_s \\ \Phi_{d_1} \\ \Phi_{d_2} \\ \Phi_{d_3} \\ \Phi_{d_4} \\ \Phi_{d_5} \end{pmatrix} = \begin{pmatrix} 1 & 0 & 0 & 0 & 0 & 0 & 0 \\ 0 & 1 & 1 & 1 & 1 & 1 & 1 \\ 0 & 1 & 0 & 0 & -1 & 0 & 0 \\ 0 & 0 & 0 & 1 & 0 & 0 & -1 \\ 0 & 0 & 1 & 0 & 0 & -1 & 0 \\ 0 & 1 & -2 & 1 & 1 & -2 & 1 \\ 0 & 1 & 0 & -1 & 1 & 0 & -1 \end{pmatrix} \begin{pmatrix} \Phi_0^+ \\ \Phi_1^+ \\ \Phi_2^+ \\ \Phi_3^+ \\ \Phi_4^+ \\ \Phi_5^+ \\ \Phi_6^+ \end{pmatrix} \equiv \hat{\chi}_s \begin{pmatrix} \Phi_0^+ \\ \Phi_1^+ \\ \Phi_2^+ \\ \Phi_3^+ \\ \Phi_4^+ \\ \Phi_5^+ \\ \Phi_6^+ \end{pmatrix} \quad (\text{A23})$$

$$\begin{pmatrix} \Phi_{p_1} \\ \Phi_{p_2} \\ \Phi_{p_3} \\ \Phi_{f_1} \\ \Phi_{f_2} \\ \Phi_{f_3} \end{pmatrix} = \begin{pmatrix} 1 & 1 & 0 & -1 & 1 & 0 \\ 1 & 0 & 1 & 1 & 0 & -1 \\ 0 & -1 & -1 & 0 & 1 & -1 \\ 0 & 1 & -1 & 0 & -1 & -1 \\ 1 & 0 & -1 & 1 & 0 & 1 \\ 1 & -1 & 0 & -1 & -1 & 0 \end{pmatrix} \begin{pmatrix} \Phi_1^- \\ \Phi_2^- \\ \Phi_3^- \\ \Phi_4^- \\ \Phi_5^- \\ \Phi_6^- \end{pmatrix} \equiv \hat{\chi}_t \begin{pmatrix} \Phi_1^- \\ \Phi_2^- \\ \Phi_3^- \\ \Phi_4^- \\ \Phi_5^- \\ \Phi_6^- \end{pmatrix} \quad (\text{A24})$$

We diagonalize the equation using

$$\hat{L}_i^{\text{diag}} = \hat{\chi}_i \cdot \hat{L}_i \cdot \hat{\chi}_i^{-1} \quad (\text{A25})$$

The respective block-diagonal self-consistent equations are

$$\begin{pmatrix} UL_0 & 2VL_1 & 0 & 0 & 0 & 0 & 0 \\ 6UL_1 & \mathcal{K}_s & 0 & 0 & 0 & 0 & 0 \\ 0 & 0 & \mathcal{K}_{d_{T_{2g}}} & 0 & 0 & 0 & 0 \\ 0 & 0 & 0 & \mathcal{K}_{d_{T_{2g}}} & 0 & 0 & 0 \\ 0 & 0 & 0 & 0 & \mathcal{K}_{d_{T_{2g}}} & 0 & 0 \\ 0 & 0 & 0 & 0 & 0 & \mathcal{K}_{d_{E_g}} & 0 \\ 0 & 0 & 0 & 0 & 0 & 0 & \mathcal{K}_{d_{E_g}} \end{pmatrix} \begin{pmatrix} \Phi_0 \\ \Phi_s \\ \Phi_{d_1} \\ \Phi_{d_2} \\ \Phi_{d_3} \\ \Phi_{d_4} \\ \Phi_{d_5} \end{pmatrix} = \begin{pmatrix} \Phi_0 \\ \Phi_s \\ \Phi_{d_1} \\ \Phi_{d_2} \\ \Phi_{d_3} \\ \Phi_{d_4} \\ \Phi_{d_5} \end{pmatrix} \quad (\text{A26})$$

$$\begin{pmatrix} \mathcal{K}_p & 0 & 0 & 0 & 0 & 0 \\ 0 & \mathcal{K}_p & 0 & 0 & 0 & 0 \\ 0 & 0 & \mathcal{K}_p & 0 & 0 & 0 \\ 0 & 0 & 0 & \mathcal{K}_f & 0 & 0 \\ 0 & 0 & 0 & 0 & \mathcal{K}_f & 0 \\ 0 & 0 & 0 & 0 & 0 & \mathcal{K}_f \end{pmatrix} \begin{pmatrix} \Phi_{p_1} \\ \Phi_{p_2} \\ \Phi_{p_3} \\ \Phi_{f_1} \\ \Phi_{f_2} \\ \Phi_{f_3} \end{pmatrix} = \begin{pmatrix} \Phi_{p_1} \\ \Phi_{p_2} \\ \Phi_{p_3} \\ \Phi_{f_1} \\ \Phi_{f_2} \\ \Phi_{f_3} \end{pmatrix} \quad (\text{A27})$$

where

$$\mathcal{K}_s = V[L_0 + 4L_1 + L_2 + 2L_3 + 4L_4]$$

$$\mathcal{K}_{d_{T_{2g}}} = V[L_0 + L_2 - 2L_3]$$

$$\mathcal{K}_{d_{E_g}} = V[L_0 - 2L_1 + L_2 + 2L_3 - 2L_4]$$

$$\mathcal{K}_p = V[L_0 + 2L_1 - L_2 - 2L_4]$$

$$\mathcal{K}_f = V[L_0 - 2L_1 - L_2 + 2L_4]$$

These are the solutions to the two-body problem at $\mathbf{P} = 0$. The 2×2 block in Eqn. (A26) corresponds to the s -symmetrical state, the next three 1×1 blocks are triply degenerate d -states of T_{2g} symmetry and the last two are another doubly degenerate d -states with the E_g symmetry. In the case of spin triplet states in Eqn. (A27), the p - and f -states are 3-fold degenerate and they belong to the T_{1u} and T_{2u} symmetry respectively.

It is possible to evaluate the exact binding threshold for the emergence of a bound state. With the symmetrized and diagonalized equations, we set the energy value as $E \rightarrow -2W = -24t$. The self-consistent equations give

$$s : \begin{pmatrix} 1 - UL_0 & -2VL_1 \\ -6UL_1 & 1 - \mathcal{K}_s \end{pmatrix} = 0 \quad (\text{A28})$$

$$d_{T_{2g}} : 1 - \mathcal{K}_{d_{T_{2g}}} = 0 \quad (\text{A29})$$

$$d_{E_g} : 1 - \mathcal{K}_{d_{E_g}} = 0 \quad (\text{A30})$$

$$p : 1 - \mathcal{K}_p = 0 \quad (\text{A31})$$

$$f : 1 - \mathcal{K}_f = 0 \quad (\text{A32})$$

Following Ref. 19, the exact solution of the Green's functions in Eqn. (A13) are

$$L_0 = -\frac{\sqrt{3}K_0^2}{8\pi^2 t} = \frac{-0.056027549298548}{t} \quad (\text{A33})$$

$$L_1 = \frac{1}{24t} - \frac{\sqrt{3}K_0^2}{8\pi^2 t} = \frac{1}{24t} + L_0 \quad (\text{A34})$$

$$L_2 = -\frac{9\sqrt{3}K_0^2}{8\pi^2 t} - \frac{3}{4t\sqrt{3}K_0^2} + \frac{2}{3t} = 9L_0 + \frac{3}{32\pi^2 t^2 L_0} + \frac{2}{3t} \quad (\text{A35})$$

$$L_3 = \frac{\sqrt{3}K_0^2}{24\pi^2 t} - \frac{1}{8t\sqrt{3}K_0^2} = \frac{1}{64\pi^2 t^2 L_0} - \frac{L_0}{3} \quad (\text{A36})$$

$$L_4 = \frac{\sqrt{3}K_0^2}{24\pi^2 t} + \frac{1}{4t\sqrt{3}K_0^2} - \frac{1}{12t} = -\frac{L_0}{3} - \frac{1}{32\pi^2 t^2 L_0} - \frac{1}{12t} \quad (\text{A37})$$

where the complete elliptic integral of the first kind $K_0 = K\left(\frac{\sqrt{3}-1}{2\sqrt{2}}\right) = 1.598142002112540$.

The binding conditions are obtained from Eqns. (A28)–(A32) to be

$$V_c^s \leq V(U) = \frac{UL_0 - 1}{UL_0\mathcal{C} - \mathcal{C} - 12UL_1^2} \quad (\text{A38})$$

where $\mathcal{C} = L_0 + 4L_1 + L_2 + 2L_3 + 4L_4 = 12L_0 + \frac{1}{2t} = -0.172330591582576/t$.

$$V_c^{d_{T_2g}} = -22.734195989010747t \quad (\text{A39})$$

$$V_c^{d_{Eg}} = -26.810644276320041t \quad (\text{A40})$$

$$V_c^p = -16.302567033831927t \quad (\text{A41})$$

$$V_c^f = -27.416574191996979t \quad (\text{A42})$$

In specific limits, the critical binding of s -states is

$$V_c^s(U=0) = -5.80280025t \quad (\text{A43})$$

$$V_c^s(U \rightarrow +\infty) = -7.8028002504t \quad (\text{A44})$$

$$U_c(V=0) = -17.84836232388t \quad (\text{A45})$$

$$U_c(V \rightarrow +\infty) = -24t \quad (\text{A46})$$

Appendix B: Pair mass in the superlight limit

Expanding the one-particle dispersion at small \mathbf{k} , one obtains

$$\varepsilon_{\mathbf{k}} \approx -12t + tb^2(k_x^2 + k_y^2 + k_z^2) = \varepsilon_0 + \frac{\hbar^2}{2m_0}(k_x^2 + k_y^2 + k_z^2), \quad (\text{B1})$$

where $m_0 = \hbar^2/(2tb^2)$ is the free particle mass.

We define six singlet dimer basis states

$$D_{i,\mathbf{n}} = \frac{1}{\sqrt{2}}(|\uparrow\rangle_{\mathbf{n}}|\downarrow\rangle_{\mathbf{n}+\mathbf{a}_i} + |\downarrow\rangle_{\mathbf{n}}|\uparrow\rangle_{\mathbf{n}+\mathbf{a}_i}). \quad (\text{B2})$$

$D_{i,\mathbf{n}}$ are the only states with nonzero weights in the $V \rightarrow \infty$ limit. Because of the topology of the FCC lattice, $D_{i,\mathbf{n}}$ are linked by first-order hopping events. The first-order Hamiltonian matrix is

$$\hat{H}D_{1,\mathbf{n}} = -t(D_{3,\mathbf{n}} + D_{3,\mathbf{n}+\mathbf{a}_6}) - t(D_{4,\mathbf{n}} + D_{4,\mathbf{n}+\mathbf{a}_5}) - t(D_{5,\mathbf{n}} + D_{5,\mathbf{n}+\mathbf{a}_4}) - t(D_{6,\mathbf{n}} + D_{6,\mathbf{n}+\mathbf{a}_3}) \quad (\text{B3})$$

$$\hat{H}D_{2,\mathbf{n}} = -t(D_{3,\mathbf{n}} + D_{3,\mathbf{n}-\mathbf{a}_5}) - t(D_{4,\mathbf{n}} + D_{4,\mathbf{n}-\mathbf{a}_6}) - t(D_{5,\mathbf{n}+\mathbf{a}_2} + D_{5,\mathbf{n}-\mathbf{a}_5}) - t(D_{6,\mathbf{n}+\mathbf{a}_2} + D_{6,\mathbf{n}-\mathbf{a}_6}) \quad (\text{B4})$$

$$\hat{H}D_{3,\mathbf{n}} = -t(D_{1,\mathbf{n}} + D_{1,\mathbf{n}-\mathbf{a}_6}) - t(D_{2,\mathbf{n}} + D_{2,\mathbf{n}+\mathbf{a}_5}) - t(D_{5,\mathbf{n}} + D_{5,\mathbf{n}+\mathbf{a}_2}) - t(D_{6,\mathbf{n}+\mathbf{a}_3} + D_{6,\mathbf{n}-\mathbf{a}_6}) \quad (\text{B5})$$

$$\hat{H}D_{4,\mathbf{n}} = -t(D_{1,\mathbf{n}} + D_{1,\mathbf{n}+\mathbf{a}_2}) - t(D_{2,\mathbf{n}} + D_{2,\mathbf{n}+\mathbf{a}_6}) - t(D_{5,\mathbf{n}-\mathbf{a}_5} + D_{5,\mathbf{n}+\mathbf{a}_4}) - t(D_{6,\mathbf{n}} + D_{6,\mathbf{n}+\mathbf{a}_2}) \quad (\text{B6})$$

$$\hat{H}D_{5,\mathbf{n}} = -t(D_{1,\mathbf{n}} + D_{1,\mathbf{n}-\mathbf{a}_4}) - t(D_{2,\mathbf{n}-\mathbf{a}_2} + D_{2,\mathbf{n}+\mathbf{a}_5}) - t(D_{3,\mathbf{n}} + D_{3,\mathbf{n}-\mathbf{a}_2}) - t(D_{4,\mathbf{n}-\mathbf{a}_4} + D_{4,\mathbf{n}+\mathbf{a}_5}) \quad (\text{B7})$$

$$\hat{H}D_{6,\mathbf{n}} = -t(D_{1,\mathbf{n}} + D_{1,\mathbf{n}-\mathbf{a}_3}) - t(D_{2,\mathbf{n}-\mathbf{a}_2} + D_{2,\mathbf{n}+\mathbf{a}_6}) - t(D_{3,\mathbf{n}+\mathbf{a}_6} + D_{3,\mathbf{n}-\mathbf{a}_3}) - t(D_{4,\mathbf{n}} + D_{4,\mathbf{n}-\mathbf{a}_2}) \quad (\text{B8})$$

Applying a Fourier transform one obtains the dimer Schrödinger equation. Its self-consistent condition yields pair energy E for a given pair momentum \mathbf{P} .

$$\begin{vmatrix} E & 0 & t(1+e^{i\mathbf{P}\mathbf{a}_6}) & t(1+e^{i\mathbf{P}\mathbf{a}_5}) & t(1+e^{i\mathbf{P}\mathbf{a}_4}) & t(1+e^{i\mathbf{P}\mathbf{a}_3}) \\ 0 & E & t(1+e^{-i\mathbf{P}\mathbf{a}_5}) & t(1+e^{-i\mathbf{P}\mathbf{a}_6}) & t(e^{i\mathbf{P}\mathbf{a}_2} + e^{-i\mathbf{P}\mathbf{a}_5}) & t(e^{i\mathbf{P}\mathbf{a}_2} + e^{-i\mathbf{P}\mathbf{a}_6}) \\ t(1+e^{-i\mathbf{P}\mathbf{a}_6}) & t(1+e^{i\mathbf{P}\mathbf{a}_5}) & E & 0 & t(1+e^{i\mathbf{P}\mathbf{a}_2}) & t(e^{i\mathbf{P}\mathbf{a}_3} + e^{-i\mathbf{P}\mathbf{a}_6}) \\ t(1+e^{-i\mathbf{P}\mathbf{a}_5}) & t(1+e^{i\mathbf{P}\mathbf{a}_6}) & 0 & E & t(e^{i\mathbf{P}\mathbf{a}_4} + e^{-i\mathbf{P}\mathbf{a}_5}) & t(1+e^{i\mathbf{P}\mathbf{a}_2}) \\ t(1+e^{-i\mathbf{P}\mathbf{a}_4}) & t(e^{i\mathbf{P}\mathbf{a}_5} + e^{-i\mathbf{P}\mathbf{a}_2}) & t(1+e^{-i\mathbf{P}\mathbf{a}_2}) & t(e^{i\mathbf{P}\mathbf{a}_5} + e^{-i\mathbf{P}\mathbf{a}_4}) & E & 0 \\ t(1+e^{-i\mathbf{P}\mathbf{a}_3}) & t(e^{i\mathbf{P}\mathbf{a}_6} + e^{-i\mathbf{P}\mathbf{a}_2}) & t(e^{i\mathbf{P}\mathbf{a}_6} + e^{-i\mathbf{P}\mathbf{a}_3}) & t(1+e^{-i\mathbf{P}\mathbf{a}_2}) & 0 & E \end{vmatrix} = 0 \quad (\text{B9})$$

The general dispersion Eqn. (B9) is too complex. However, to extract a pair mass it is sufficient to know $E(\mathbf{P})$ at small \mathbf{P} . Utilizing the isotropy property of cubic dispersion relations, we set $\mathbf{P} = (P_x, 0, 0)$ and expand Eqn. (B9) to get

$$E^3(E - 4t) \left[E^2 + 4tE - 16t^2 \left(1 + \cos \frac{P_x b}{2} \right) \right] = 0, \quad (\text{B10})$$

which defines dispersion of six pair bands along the P_x direction. The lowest band is

$$E_1(P_x) = -2t \left(1 + \sqrt{5 + 4 \cos \frac{P_x b}{2}} \right). \quad (\text{B11})$$

Expanding at small P_x , one obtains

$$E_1(P_x b \ll 1) \approx -8t + \frac{1}{6} t(P_x b)^2 \equiv E_0 + \frac{\hbar^2 P_x^2}{2m^*}, \quad (\text{B12})$$

from where

$$m^* = \frac{3\hbar^2}{tb^2} = 6m_0. \quad (\text{B13})$$

Thus even an infinitely bound intersite pair is only six times heavier than a free particle.
